

ABSTRACT

Title of Document: COMPARING LEVELS OF NDH-1
DEHYDROGENASE ACTIVITY IN
DIFFERENT MYCOBACTERIAL SPECIES.

Sharon Azogue, Master of Science, 2008

Directed By: Dr. Volker Briken, Department of Cell Biology
and Molecular Genetics

The *nuoG* gene of *Mycobacterium tuberculosis* (Mtb) has the ability to inhibit host cell apoptosis. This ability is a virulence factor and does not exist in facultative pathogenic and non-pathogenic mycobacterial species. NuoG is part of the NDH-1 complex, and this study addressed the potential link between the role of NuoG in apoptosis inhibition and the biochemical activity of the NDH-1 complex. Different mycobacterial species were tested for their NDH-1 activities. Among the bacteria tested were bacteria transformed with the Mtb *nuoG* plasmid, or with the almost entire NDH-1 coding region. Surprisingly, the levels of NDH-1 activity did not correlate with apoptosis levels, suggesting a potential independent, novel mechanism by which NuoG inhibits host cell apoptosis.

COMPARING LEVELS OF NDH-1 DEHYDROGENASE ACTIVITY IN
DIFFERENT MYCOBACTERIAL SPECIES.

By

Sharon Azogue

Thesis submitted to the Faculty of the Graduate School of the
University of Maryland, College Park, in partial fulfillment
of the requirements for the degree of
Master of Science
2008

Advisory Committee:
Dr. Volker Briken, Chair
Dr. Kevin McIver
Dr. Vincent Lee

© Copyright by

Sharon Azogue

2008

Dedication

I would like to dedicate my work to all the animals that have been sacrificed in the name of science. May their contribution to science be honored and may the moral obligation of humane practices be at the center of scientific communities around the world.

Acknowledgements

I would like to thank my advisor Volker Briken for all of his support and guidance. Working in his lab has been an inspiring example of how an advisor can maintain a position of authority while treating students with respect and care. I would like to thank my wonderful lab members for their help, advice and above all- friendship. I will miss all of you and will always cherish the time we spent together.

Jessica- you have taught me a lot about scientific methods and have always been a source of information concerning recent papers, theories behind models, the research of our colleagues and a lot more. I am especially grateful for your help with the electroporations and western blotting. Amro- you have been a source of 7H9, tween, glycerol, and a lot of other reagents I've been stealing from your bench. But more importantly, you taught me how to use several soft wares , helped me with presentations and have been my IT person. For that I am eternally grateful. Serdar- thank you for all your help with ordering, teaching me about different reagents and reviewing protocols with me. I am sorry for the Salma Hayek prank. You were right- it wasn't funny. Ben- thanks for being willing to help out whenever needed. Hana- thanks for making fun of my new career choice. Just kidding- you are awesome and I wish you good luck with your experiments. Nora, my hard-working undergrad, thank you for all your help, especially with the cloning. I am sure you have a bright future ahead of you.

I would like to thank my parents for supporting my decision to move to the US to pursue my education. Lastly, I would like to thank my wonderful husband David for supporting me in following my dreams, no matter where they take us.

Your unconditional love and your dedication make even the greatest challenges and disappointments bearable. I love you.

Table of Contents

Hypothesis and Aims.....	1
Chapter 1: Introduction.....	2
Mycobacterium tuberculosis.....	2
Mycobacterial infection.....	3
Mycobacteria and apoptosis.....	3
Mycobacterial proteins involved in apoptosis inhibition.....	4
Gain-of-function genetic screen for anti-apoptosis genes in Mtb.....	5
Figure 1.....	8
Figure 2.....	9
The mycobacterial <i>nuoG</i> gene.....	10
Figure 3.....	12
The mechanism of apoptosis inhibition by Mtb.....	13
Reactive oxygen species (ROS) and apoptosis.....	13
Figure 4.....	14
Working model.....	16
Figure 5.....	17
Chapter 2: Results.....	18
Membrane isolation.....	18
Establishing the NDH activity assays.....	18
Figure 6.....	19
Figure 7.....	20
Performing NDH activity assays.....	21
Figure 8.....	24
Figure 9.....	25
Figure 10.....	26
Figure 11.....	27
Figure 12.....	28
Figure 13.....	29
Figure 14.....	30
Figure 15.....	31
Figure 16.....	32
Creation of myc-tagged and un-tagged <i>nuoG</i> plasmids.....	33
Creation of BCG Δ <i>nuoG</i> bacteria transformed with myc- <i>nuoG</i>	33
Creation of Mtb Δ <i>nuoG</i> bacteria transformed with myc- <i>nuoG</i>	33
Creation of plasmids for full-length and partial Mtb <i>nuoG</i> antibody.....	34
Figure 17.....	35
Figure 18.....	36
Figure 19.....	37
Chapter 3: Discussion.....	38
Chapter 4: Experimental procedures.....	42
Appendix 1.....	49

Appendix 2.....	50
Bibliography.....	51

List of Figures

Figure 1 : <i>nuoG</i> is an anti-apoptosis gene of Mtb	14
Figure 2 : <i>nuoG</i> is a virulence gene in Mtb	15
Figure 3 : NuoG is part of the NDH-1 complex and is not secreted	18
Figure 4 : <i>nuoG</i> is important for inhibiting apoptosis induction	20
Figure 5 : Working Model.....	23
Figure 6 : NDH-1 activity Msmeg.....	25
Figure 7 : NDH-1 membrane titration.....	26
Figure 8 : Deletion of <i>nuoG</i> abolishes NDH-1 activity.....	30
Figure 9 : NDH-1 assays for BCG, Mkans, neg. control, and inhibitor.....	31
Figure 10 : NDH-1 activity BCG, Mkans.....	32
Figure 11 : NDH-1 assays of Msmeg, Msmeg+ <i>nuoG</i> , Msmeg+J21.....	33
Figure 12 : Comparing NDH-1 activities of Msmeg, Msmeg+ <i>nuoG</i>	34
Figure 13 : Comparing levels of NDH-1 activity.....	35
Figure 14 : NDH-2 activity for Mkans, BCG, and neg. control	36
Figure 15 : NDH-2 activities of Msmeg, Msmeg+ <i>nuoG</i> , Msmeg+J2.....	37
Figure 16 : Comparing levels of NDH-2 activity.....	38
Figure 17 : Map of the Mtb- <i>nuoG</i> antibody plasmid	41
Figure 18 : <i>nuoG-myc</i> genes in pmv261.....	42
Figure 19 : Mtb NuoG-Myc proteins are expressed in Mtb Δ <i>nuoG</i>	43

Hypothesis

Enzymatic activity of NDH-1 is related to anti-apoptotic capacity of the NuoG subunit of NDH-1 and to virulence in *mycobacteria*.

Aims

- 1) Correlate NDH-1 enzymatic activity of various mycobacterial species with pathogenicity. This aim can support the hypothesis that high NDH-1 activity is related to a high degree of virulence in *mycobacteria*.
- 2) Correlate NuoG proteins from different *mycobacteria* with NDH-1 enzymatic activity. This will be done by analyzing enzymatic activity in bacteria containing the TB *nuoG* plasmid, and the cosmid containing almost the entire TB *nuo* operon (“gain of function”). This aim can demonstrate whether NuoG of the virulent Mtb will result in higher NDH-1 activity when transformed into less virulent mycobacterial species.
- 3) Create molecular tools for future NDH-1 activity studies of the different mycobacterial *nuoG* proteins. This will be done by creating *nuoG* plasmids (myc-tagged and untagged) of different *mycobacteria* to be used in NDH activity studies and apoptosis assays. These plasmids can be transformed into BCG Δ *nuoG* and TB Δ *nuoG* bacteria in order to compare the impact of the different mycobacterial *nuoG* proteins on NDH-1 enzymatic activity. Creating an antibody against NuoG will serve as a tool to study the localization of NuoG and therefore verify that NuoG acts only as a subunit of NDH-1, and does not have a function that is separate from enzymatic activity.

Chapter 1: Introduction

Mycobacterium tuberculosis

The global importance of tuberculosis (TB) is enormous and constantly growing. Currently, about one third of people are infected with TB, and it is estimated that 2.5 million people die of TB annually (Dye 2005). The HIV epidemic provides large numbers of easy human targets, as HIV positive individuals are extremely prone to reactivation of latent TB infections (Barnes 1994). Multi-drug resistant (MDR) strains of Mtb have surfaced in 70 countries, with 400,000 new cases occurring each year (Jacobs 2003, Matteelli 2007). Extreme-drug resistant (XDR) strains have been increasingly emerging worldwide. An XDR TB outbreak that occurred in South Africa in 2007 resulted in 52 deaths out of 53 cases within 16 days (Singh 2007).

The chemotherapy of Mtb includes a combination of strong antibiotics taken daily for a period of 6-9 months. In addition to potential side effects such as liver damage, the drugs efficacy is decreasing as the number of MDR and XDR cases are increasing. The live vaccine strain used against TB is Bacillus Calmette-Guerin (BCG) and was derived from a virulent bovine strain called *M. bovis*. This vaccine has been used for the past 87 years, and although it is safe it is highly inefficient and only protects 0-80% of vaccinated individuals, depending on their country of origin.

Mycobacterial infection

Mtb initially infects the alveolar macrophages in the lungs, and can be spread via aerosolized droplets to uninfected individuals (Jacobs 2003). The bacteria multiply within the macrophage and then disseminate throughout the body. Once the adaptive immune response is activated, the bacterial burden is controlled in 90% of infected individuals. These individuals are considered to have a latent infection, with a low number of TB bacilli persisting in their lungs.

Mycobacteria and apoptosis

Although macrophages have the ability to destroy the majority of invaders, Mtb is able to persist and to replicate within the host macrophage. Mtb has the ability to manipulate its host cells on many levels. One example is the role of the mycobacterial cell-wall lipids and mycobacterial protein kinase G in inhibition of phagosome maturation (Walburger 2004, Pethe 2004). The research in my lab addresses the ability of Mtb to influence host cell apoptosis.

The induction of apoptosis following infection by a pathogen is highly conserved among the animals and plant kingdoms (Abramovitch 2004, Iriti 2007). Since apoptosis plays an important role in the innate immune response against pathogens, it is essential for a pathogen to combat apoptosis in order to persist. One study showed that apoptotic cell death reduced the viability of the mycobacteria, whereas necrotic cell death did not (Pan 2005). Apoptosis also plays a big role in initiating an adaptive immune response against Mtb. Phagocytosis of Mtb apoptotic bodies by dendritic cells (DCs) causes presentation of peptide antigens, leading to

specific T cell activation (Schaible 2003). In addition, cross priming occurs as extra-cellular antigens are presented on MHC I molecules and activate cytolytic T cells (Guermonprez 2005).

There are contradictory reports about the outcome of Mtb in regards to apoptosis. Several reports show that virulent Mtb induces apoptosis in host cells, while others show inhibition of apoptosis by Mtb. These differences can be reconciled by understanding the complexity of the experimental system that depends on many variables. For example, primary alveolar macrophages obtained from Mtb infected individuals showed a higher level of macrophage apoptosis when compared to macrophages from healthy individuals (Klingler 1997, Placido 1997). However, there is increasing evidence that virulent Mtb inhibits host cell apoptosis. One study showed that virulent species of *Mycobacteria*, such as Mtb Erdman and *M.bovis*, induced much lower levels of apoptosis in primary human alveolar macrophages than non-virulent mycobacterial species, such as BCG and *M.smegmatis* (Keane 2000).

Mycobacterial proteins involved in apoptosis inhibition

The Mtb protein SecA2 is implicated in the inhibition of apoptosis. SecA2 codes for a secretion system that mediates secretion of superoxide dismutase A (SodA), an enzyme that catalyzes the conversion of superoxide ions to hydrogen peroxide. SecA2 deletion mutants induced more apoptosis than wild-type Mtb (Braunstein 2003). A second protein involved in host apoptosis inhibition is protein kinase E (PknE). PknE is a serine threonine kinase whose promotor is induced

during nitric oxide (NO) stress. PknE deletion mutants were more susceptible to NO, and also exhibited higher levels of apoptosis (Jayakumar 2007). A third protein, nuoG, inhibits host cell apoptosis and is the subject of my research.

Gain-of-function genetic screen for anti-apoptotic genes in Mtb:

To identify the genes in Mtb that are behind the anti-apoptotic phenotype, a gain-of-function genetic screen was established using the non-pathogenic *M.smegmatis* mc² 155 strain (Msmeg). This strain is fast growing and highly transformable. The host cell used was the human cell line THP-1, which in publications was shown to be an accurate model for the apoptotic response of Mtb-infected primary human alveolar macrophages (Reindeau 2003). The gain-of-function was performed using a library of 312 *M.smeg* clones containing Mtb genomic DNA fragment on an episomal cosmid. The two clones, “J21” and “M24”, which contained non-overlapping Mtb genomic DNA inserts, showed the most significant reduction in apoptosis (appendix 1).

The two cosmids were then transformed into *M. kansasii* (Mkans), an opportunistic pathogen and strong (yet slow) inducer of apoptosis. Based on fluorescence activated cell sorter (FACS) analysis and terminal deoxynucleotidyl transferase dUTP nick end labeling (TUNEL) staining, wild type Mkans and Mkans with the empty cosmid vector (CO) induced high levels of apoptosis at 5 days post infection (95% and 86%, respectively). Mkan-J21 and Mkan-M24 showed significantly reduced levels of apoptosis (16% and 19%, respectively) (Figure 1). The transfection of the two cosmids into *M.Kansasii* and *M.Smegmatis* did not

affect in vitro growth. In vivo, Mkan-J21 and Mkan-M24 showed significantly increased virulence in SCID mice (44 d and 60 d respectively, verses >200 d for the Mkan-CO) (Figure 2).

The Mkan-J21 was chosen for further studies, as it induced higher virulence in SCID mice than the Mkan-M24. The Mkan-J21 cosmid contained almost the entire *nuo* operon (with half of *nuoA* missing), which encodes for the 14 subunit Mtb type I NADH dehydrogenase complex (NDH-1), along with other known-function and predicted-function genes. To identify which genes conferred the anti-apoptotic phenotype, a series of deletion mutants was created in Mtb H37Rv (virulent strain) using specialized transduction (Bardarov 2002). While several deletion mutants showed modest effect on virulence in SCID mice and loss of apoptosis with THP-1 cells, the mutant with the deletion of the *nuoG* gene showed significant differences. The region of the cosmid named “7/10” also induced apoptosis when deleted (unpublished), but to a lesser degree than *nuoG*. Using reverse transcriptase-PCR the transcription of *nuoG* from the J21 cosmid in *M.smegmatis* was confirmed. A complementation was performed using the plasmid carrying *nuoG* behind a constitutively active promoter that integrates into the Mtb chromosome at a unique attB site (Stover 1991). The complementation verified that there are no polar effects of the deletion on nearby genes, and gave full complementation for the in vitro assays (Figure 1 C).

The difference in apoptosis induction was proven to not be a result of reduced phagocytosis of the *nuoG* mutant. This was shown by comparing rates of infection via acid-fast staining and CFU determination. The Mtb Δ *nuoG* mutant still

induced less apoptosis than *M.Kansasii* in THP-1 cells and cultured primary mouse cells, probably due to the fact that Mtb has multiple anti-apoptotic genes.

Figure 1

nuoG is an anti-apoptosis gene of *Mtb*

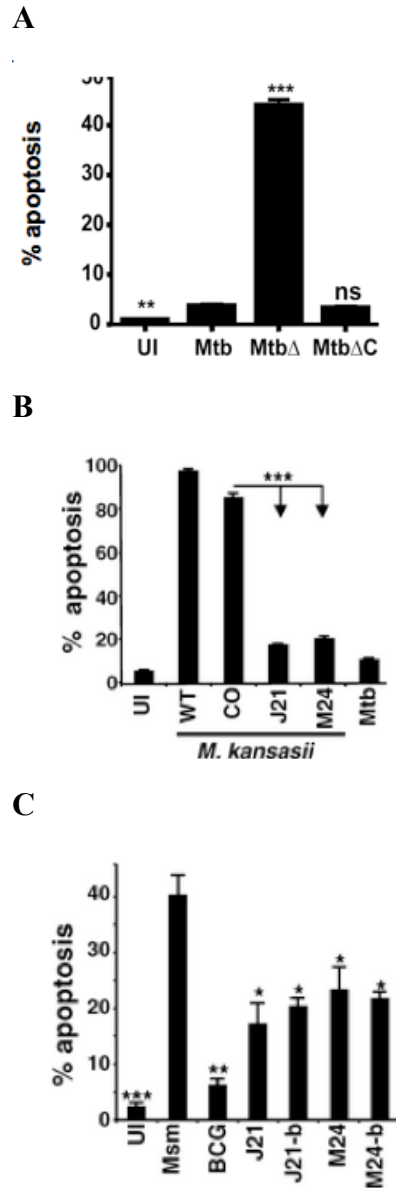
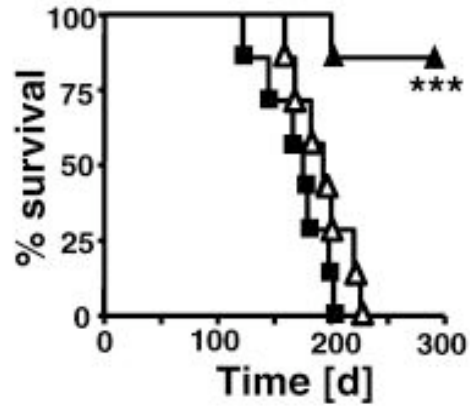


Figure 1. *nuoG* is an anti-apoptosis gene of *Mtb*. Induction of apoptosis by infection of differentiated human THP-1 cells with wild type (*Mtb*), the *nuoG* deletion mutant (*Mtb* Δ *nuoG*), or complemented mutant (*Mtb* Δ C). Cells were harvested at day 3 after infection, stained by tunnel assay and analyzed using flow cytometry (A). The J21 and M24 cosmids and empty vector cosmid (CO) were transfected into *M. kansasii*, and the induction of apoptosis was compared to uninfected and *Mtb*-infected THP-1 cells using TUNEL at day 5 post-infection (B). *M. smegmatis* was transfected with the J21 and M24 cosmids, as well as with the purified and re-transfected J21-b and M24-b clones. The clones, original transformants, uninfected cells (UI), *M. smegmatis* (Msm) and BCG were tested for apoptosis induction following infection of THP-1 cells, TUNEL staining 16 h post-infection, and flow cytometry (C) (Briken 2007)

Figure 2

nuoG is a virulence gene in Mtb

A



B

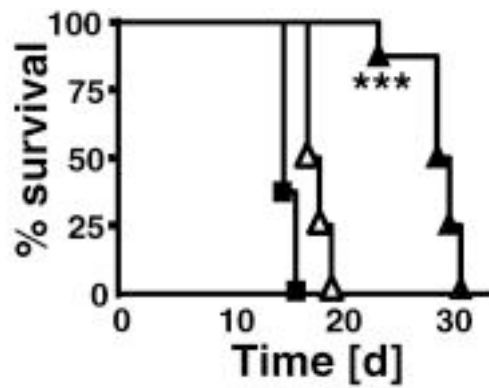


Figure 2. Survival of immunocompetent BALB/c mice after intravenous infection with 10^6 wild type Mtb (squares), MtbΔnuoG (filled triangles), or complemented MtbΔnuoG (empty triangles). n=7 mice per group (A). Survival of SCID mice infected with the bacterial strains as in A. n=7 mice per group (B) (Briken 2007)

The mycobacterial *nuoG*

The first anti-apoptotic gene that was identified by our lab, *nuoG*, is a part of the *nuo* operon and codes for a protein NDH-1. NDH-1 is a proton-pumping NADH ubiquinone reductase, and is also called respiratory complex 1. It is the first enzyme of the bacterial and mitochondrial respiratory chain. It catalyzes the transfer of two electrons from NADH to quinone, coupled with the translocation of four protons across the membrane (Sazanov 2006, Walker 1992). The mitochondrial complex contains 46 proteins, whereas the bacterial complex contains 14 (Matsuno-Yagi 2003). The structure of the NDH-1 of mycobacteria hasn't been studied. However, extensive research has been conducted on the analogous *E.coli* NDH-1. Electron microscopy showed that both the bacterial and mitochondrial enzyme have an L shaped structure (Sazanov 2003) (Figure 3 A and B). The peripheral hydrophilic domain contains flavin-mononucleotide (FMN), the NADH-binding site, and eight or nine iron-sulfur (Fe-S) clusters. The membrane embedded domain contains the proton-pumping machinery. FMN accepts two electrons simultaneously (as a hydride) from NADH and transfers them one by one to the electron carriers, the Fe-S clusters. These reduce the membrane-embedded quinone to quinol in two one-electron steps (Matsuno-Yagi 1997, Finel 2001).

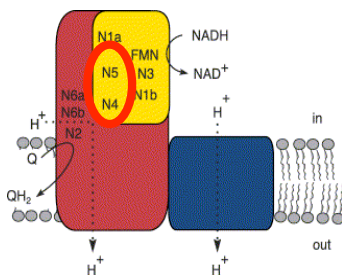
Mtb has two additional non-proton pumping type II NADH dehydrogenases encoded by the *ndh* and the *ndhA* genes. This supports the evidence that NDH-1 is not essential for mycobacterial growth in culture. Sequence comparisons revealed that *nuoG* of Mtb is 99.9% homologous to that of BCG, 70% identical to that of *M.smegmatis*, and 58% identical to that of *M.kansasii*.

To determine whether *nuoG* is secreted and effects cell signaling directly, a *phoA-nuoG* fusion protein was created. This protein, if secreted, can convert a colorless substrate to blue. The assay did not show that *nuoG* is secreted (Miller et. al unpublished, Figure 3 C). Supporting this conclusion is the fact that NuoG lacks a signal peptide and has a predicted cytosolic location. If the structure of the mycobacterial Ndh-1 is similar to that of other bacterial Ndh-1 complexes (such as *E.coli*), the NuoG is located on the peripheral arm of the complex and is cytoplasmic.

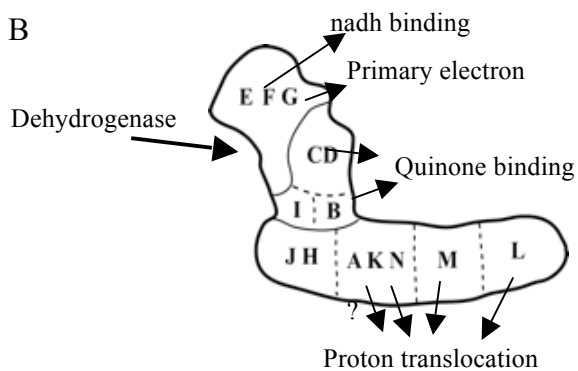
Figure 3

NuoG is part of the NDH-1 complex and is not secreted

A



B



C

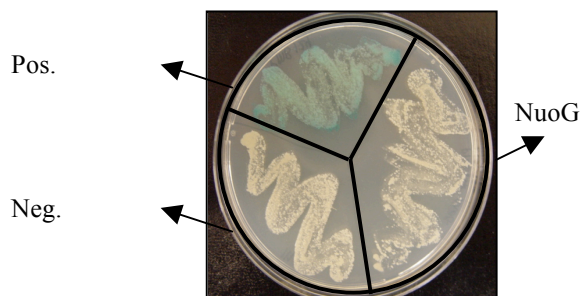


Figure 3. Cartoon representation of the NDH-1 complex. NuoG is in yellow (A). Diagram of the NDH-1 complex with the sub-units labeled for function/ predicted function (B). The *nuoG-phoA* fusion protein expressed in *M. smegmatis*. If the protein is secreted it turns the colorless substrate blue (Miller et. al unpublished) (C).

The mechanism of apoptosis inhibition by Mtb

Mtb can inhibit apoptosis via both the intrinsic and the extrinsic pathways. A study showed that inhibition of the intrinsic/ mitochondria-mediated pathway can involve the BCL-2 like genes *mcl-1* and *A1* (Spratt 2005). Another study showed that caspases 8 and 10, which are involved in the extrinsic/ death receptor-mediated pathway, were activated following Mtb infection (Braunstein 2000). Therefore, Mtb probably inhibits apoptosis via multiple pathways.

NuoG inhibits apoptosis via the extrinsic pathway. Experiments performed in our lab by Jessica Miller showed that *nuoG* inhibition of apoptosis is dependant on caspase 8 (extrinsic pathway) but not caspase 9 (intrinsic pathway). Additional experiments performed by Miller showed that TNF- α mediated the Mtb Δ *nuoG* induction of apoptosis, TNF- α secretion was ROS dependant, and ROS were generated by the bacterial NADPH oxidase complex (NOX2). One study done by Miller showed that in macrophages with a deletion of the *gp91* that results in an inactive NOX2 complex, deleting *nuoG* does not abolish apoptosis inhibition (Miller et. Al unpublished, Figure 4).

Reactive Oxygen Species (ROS) and apoptosis

The mechanism of apoptosis inhibition by *nuoG* involves targeting the reactive oxygen species (ROS) created by the host cell phagocyte NADPH oxidase (NOX2) (Briken 2007). NOX2 is a multi subunit complex that become recruited and activated onto the phagosomal membrane upon phagocytosis of pathogens (Purdy 2005, Behr 1999). It oxidizes NADPH in the cytosol to NADP⁺, and

reduces oxygen in the lumen to superoxide. The superoxide, which is very reactive and bactericidal, will generate further ROS. An increase in ROS in the lumen might cause an increase in ROS to the cytosol and cause change in TNF-alpha signaling from survival to cell death. The increase in cytosolic ROS can trigger inactivation of the MAP Kinase Phosphatase (MKP), resulting in sustained Jun N-terminal Kinase (JNK) activation.

Figure 4

nuoG is important for inhibiting NOX2 mediated apoptosis induction

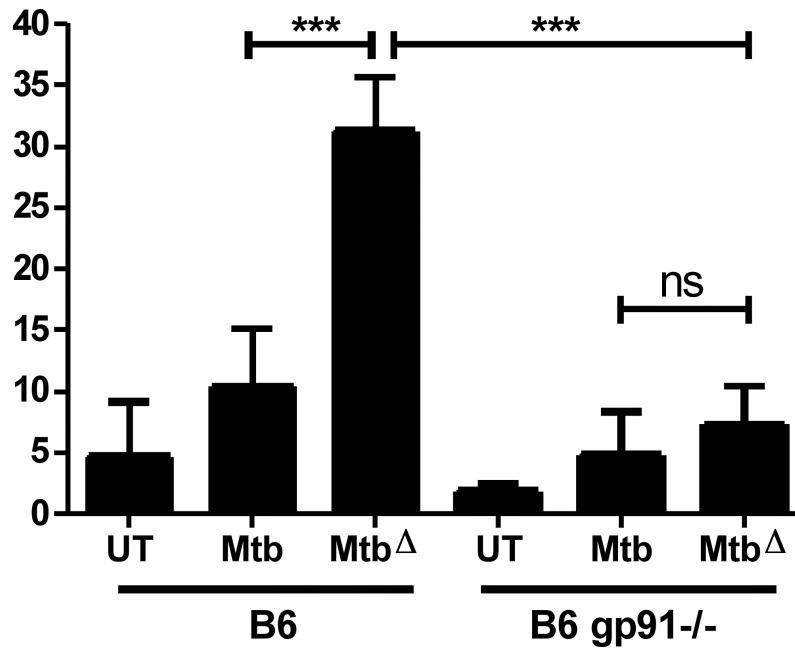


Figure 4. Macrophages derived from C57B1/6 and gp91-KO mice were infected with Mtb and MtbΔ*nuoG*. The gp91 mice have an inactive NOX2 complex. The cells were infected for 4 h, chased for 24 h, then TUNEL stained. Apoptosis was measured by flow cytometry (Miller et. al unpublished).

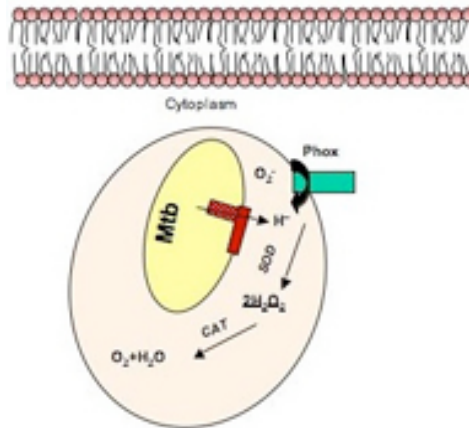
Working model

The model for the *nuoG*-mediated inhibition of host cell apoptosis proposed by our lab is as follows. Upon phagocytosis of bacteria, NOX2 gets recruited to the phagosomal membrane and activated. The NOX2 generate a lot of ROS, which are extremely bactericidal. The NDH-1 complex neutralizes the ROS by pumping protons into the phagosomal lumen, which then quickly react with the superoxide . The reaction is catalyzed by the bacterial superoxide dismutase enzyme (SOD). The reaction generates hydrogen peroxide, which is then transformed into water and oxygen by another reaction, catalyzed by the bacterial catalase enzyme. We hypothesize that deleting *nuoG* creates a non-functional NDH-1. If the NDH-1 does not neutralize the superoxide it reacts with other substrates to generate ROS. The ROS will accumulate until it will leak into the cytosol of the host cell. High levels of cytosolic ROS can activate JNK and also induces an increase in TNF- α . The increase in TNF- α creates a positive feed-back loop, with the secreted TNF- α binding to its receptor and leading to more JNK activation. Activated JNK leads to pro-apoptotic signal transduction.

Figure 5

Working model

A



B

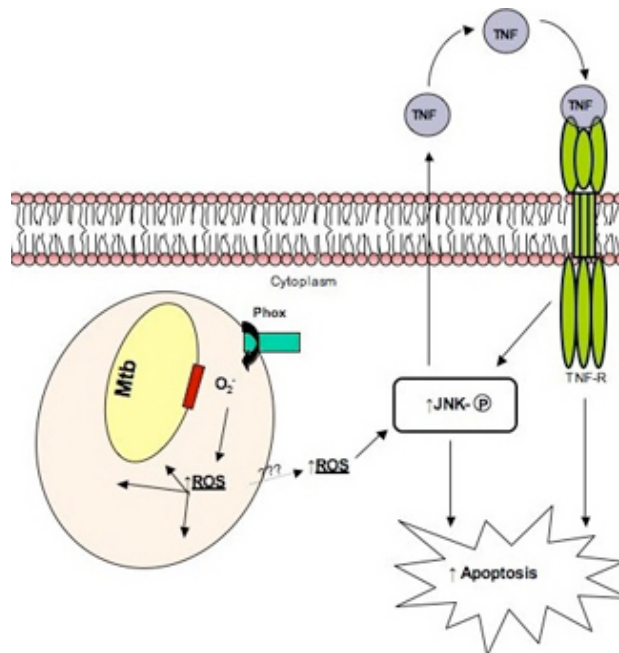


Figure 5. In the wild type bacteria, NDH-1 (containing NuoG) pumps protons into the phagosomal lumen. The protons react with the superoxide in a reaction catalyzed by the bacterial superoxide dismutase (SOD). Hydrogen peroxide is generated, which is then transformed into water and oxygen in a reaction catalyzed by the bacterial catalase (Miller et al unpublished) (A). In the *nuoG* deletion mutant NOX2 (Phox) gets recruited and activated upon phagocytosis of bacteria. This increases the amount of superoxide in the phagosome, leading to the generation of bactericidal ROS. The ROS leaks into the cytosol of the macrophage, activates JNK and leads to a pro-apoptosis signaling cascade via increase in TNF- α (B).

Chapter 2: Results

Membrane isolations

In order to study the NDH-1 activities of the different mycobacterial species, membranes were isolated from one, two, or three separate preps of BCG, Mkans, Msmeg, Msmeg+ J21, and Msmeg+ pmv261-nuoG. Membrane isolations were performed via ultra-centrifugation, following the breaking of the bacteria with a French-press (see material and methods).

Establishing the NDH activity assays

Different titrations of membrane preps and Nhdh/ Nadh substrates were tested to establish the optimal conditions for the experiment. The titrations revealed that 20 μ l of 0.8 μ g/ml membrane preps achieved comparable results to double and triple the amounts of membrane preps. Since the final amount of membrane preps produced from 500 ml bacterial cultures were small, 20 μ l of membranes were established as the standard for all experiments (Figure 6). Using 20 μ l of 20 μ M Nhdh/Nadh achieved significant NDH-1/ NDH-2 activity. Doubling and tripling the amounts of nhdh/nadh achieved higher activity readings, however the correlation was not linear. Since the Nhdh is extremely expensive, using 20 μ l of Nhdh/Nadh was established as the standard (Figure 7).

Figure 6

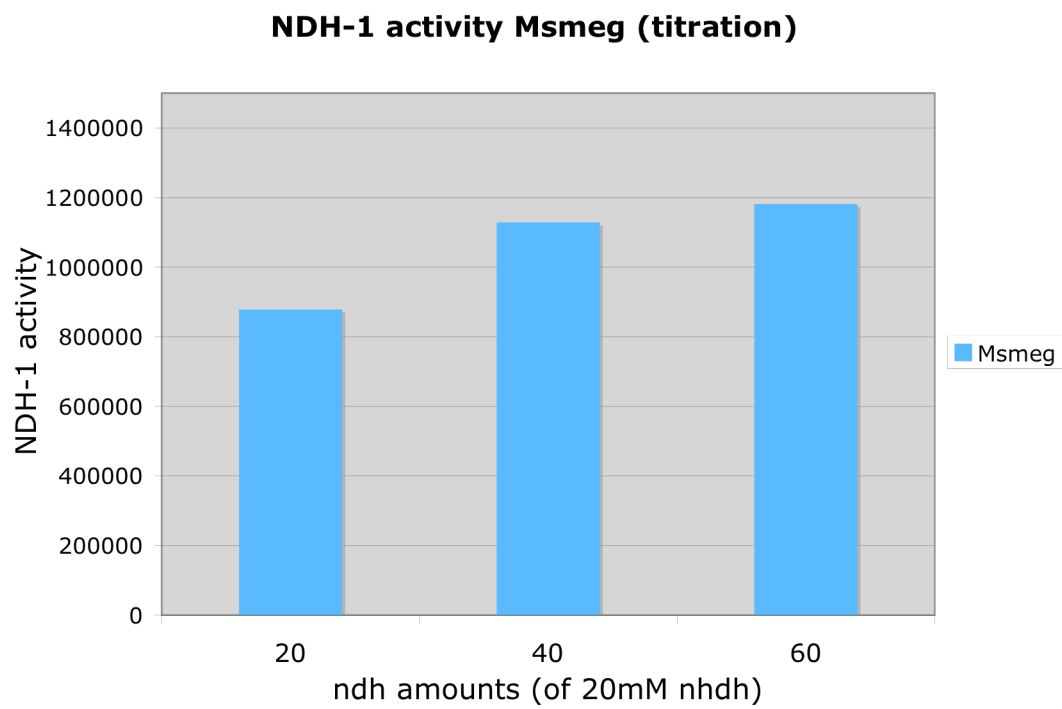


Figure 6. 20, 40, and 60 μ l of 20 mM Nhdh were used to calculate NDH-1 enzymatic activity in *M.smegmatis*. Activity is shown as mol/min/mg.

Figure 7

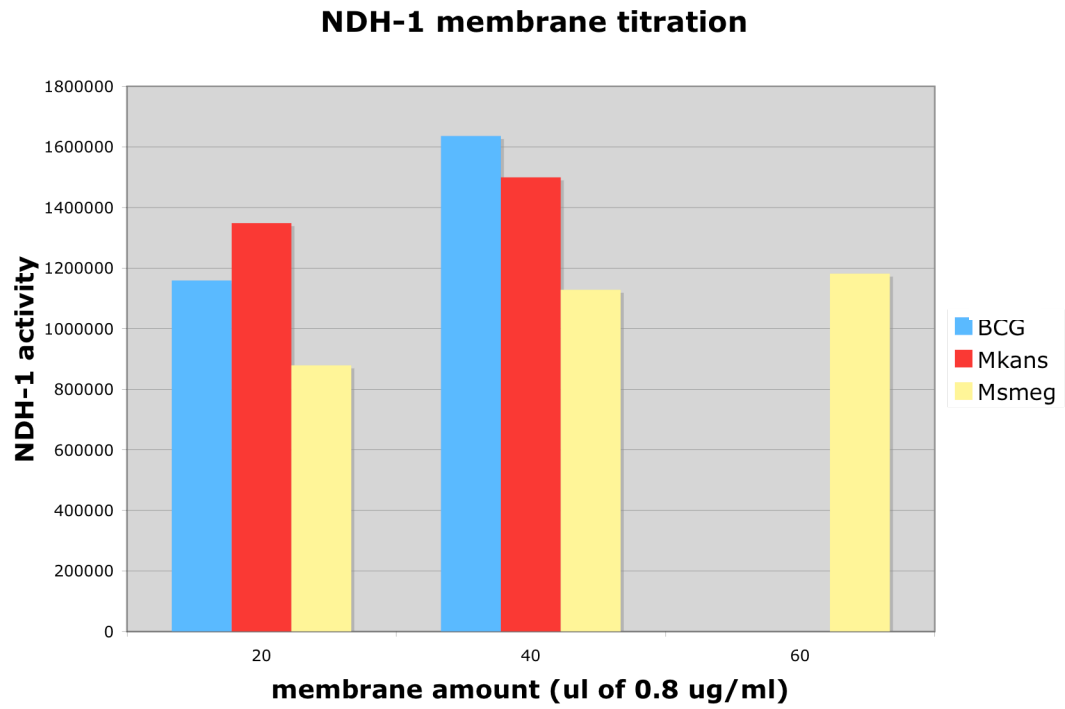
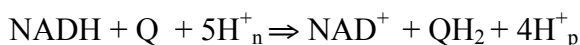


Figure 7. 20, 40, and 60 µl of 0.8 µg/ml membrane preps were used to calculate NDH-1 enzymatic activity. Activity is shown as mol/min/mg.

Performing NDH-1 and NDH-2 activity assays

In order to compare the NDH-1 and NDH-2 activities of the different *mycobacteria*,

NDH-1 and NDH-2 assays were performed (see material and methods for a detailed protocol). NADH reduction occurs according to the following formula.



Q- quinone. H^+_{n} , H^+_{p} – the protons taken from the negative inner side to the positive outer side.

NADH is a substrate specific for NDH-2 activity, and NHDH is a substrate specific for NDH-1 activity (Appendix 2). The two substrates are structurally similar, the only difference being that NHDH has a carbonyl where NADH has an amine. DCIP was used as a substrate in place of quinone, and reduction of DCIP was measured by plotting OD over time as the blue substrate turned colorless. Assays were performed in triplicates for all of the above mentioned membrane preps. Kinetic slopes were obtained and used to calculate the enzymatic biochemical activities.

A previous experiment performed by collaborator Catherine Vilcheze from the Albert Einstein school of Medicine, revealed that deleting *nuoG* abolished the NDH-1 activity of BCG, but not the NDH-2 activity (Figure 8). My experiments were designed to measure NDH-1 activities and correlate them with the endogenous NuoG proteins of the different bacteria, as well as test for “gain of function” following transformation with a *Mtb nuoG* plasmid or a cosmid containing *Mtb*

nuoG. The raw data is presented in the form of the NDH-1 kinetic slopes (Figures 9 and 11).

Potassium cyanide was used to inhibit the reaction, and had an activity value close to zero. As a negative control, the experiment was performed using water instead of membrane preps, and the resulting activity was three-fold lower than activities of BCG and Mkans NDH-1 enzymes (Figure 10). The NDH-1 activities of BCG and Mkans were not significantly different, indicating that the low-apoptosis inducing BCG has similar NDH-1 activity to the high-apoptosis inducing Mkans. In NDH-1 experiments performed in Msmeg, Msmeg+*nuoG*, and Msmeg+ J21, the enzymatic activities proved to be similar (Figure 12). This result indicates that no enzymatic “gain of function” was observed when adding the *nuoG* or the *nuo* operon of low-apoptosis inducing Mtb to high-apoptosis inducing Msmeg. The NDH-1 activities of all the Msmeg bacteria were low- approximately 50% higher than the activity of the negative control (water).

When comparing the NDH-1 of the facultative pathogenic BCG and Mkans, to the non pathogenic Msmeg bacteria (with and without plasmids/ cosmids), it appears that the activity of the facultative pathogenic BGC and Mkans is two fold higher than that of the non pathogenic Msmeg bacteria, and three-fold higher than the negative control activity (Figure 13).

Levels of NDH-2 activity of the different *mycobacteria* were measured as a control. NDH-2 is a non-proton pumping NADH dehydrogenase that has no correlation with host cell apoptosis and was therefore expected to have similar activities in the different *mycobacteria*. The kinetic slopes were found to be similar

in all the *mycobacteria* tested (Figures 14 and 15). The NDH-2 activities of the different *mycobacteria* were found to be similar as well (Figure 16).

Figure 8

Deletion of *nuoG* abolishes NDH-1, but not NDH-2 enzymatic activity

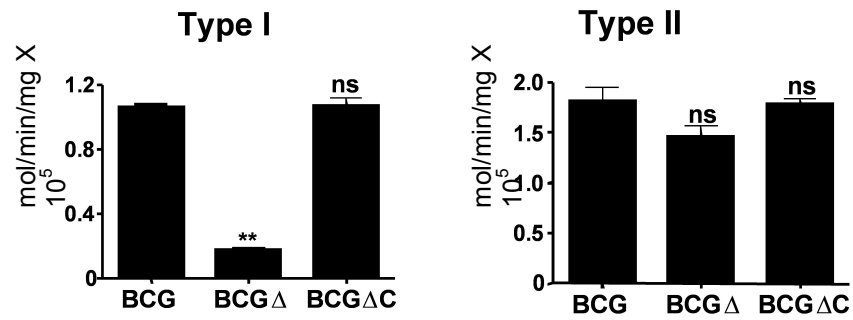


Figure 8. Membrane fractions of BCG, BCG Δ *nuoG*, and complemented BCG (BCG Δ C) were isolated. The membrane fractions were tested for type 1 and type 2 activities. (Vilcheze et. al unpublished).

Figure 9

NDH-1 assays for BCG, Mkans, neg. control, and inhibitor

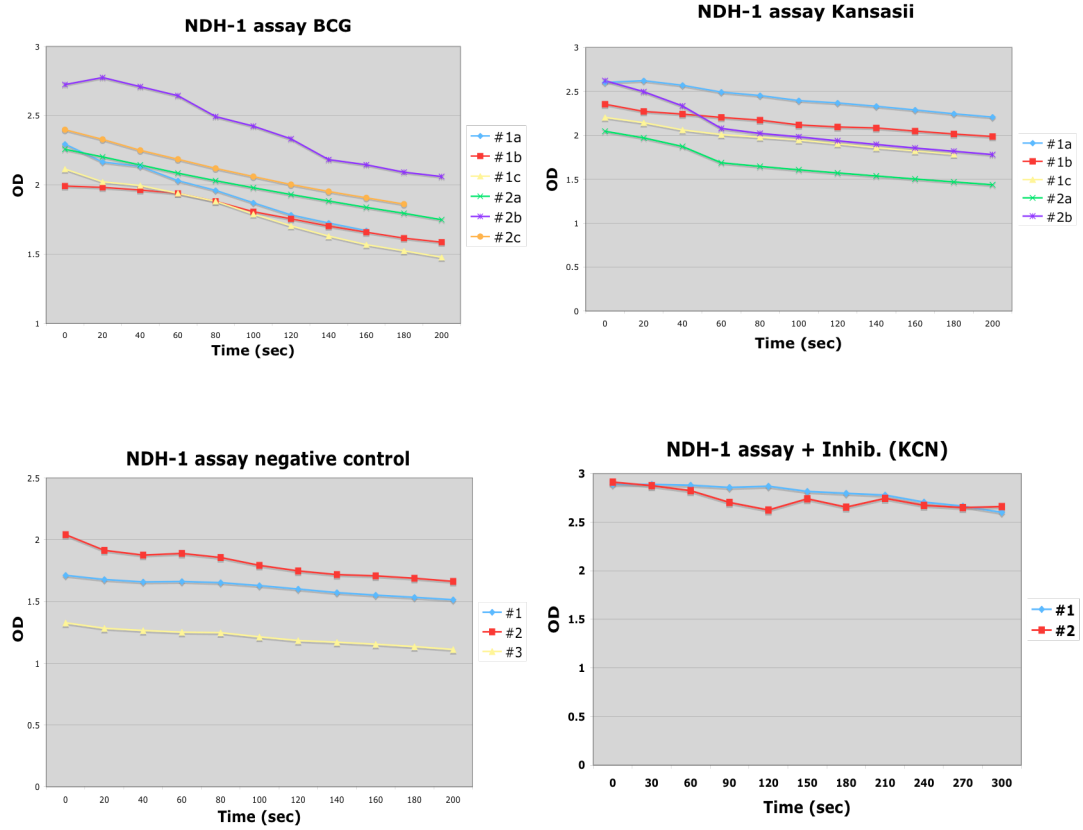


Figure 9. Kinetic slopes for NDH-1 assays are shown as reduction of OD over time. Kinetic slopes were measured following the addition of the DCIP substrate to BCG, Mkans, phosphate buffer (neg. control), or phosphate buffer with 20 mM KCN (inhibitor of the reaction). Different colored lines indicate separate reactions and different numbers indicate separate membrane isolations for the bacteria.

Figure 10

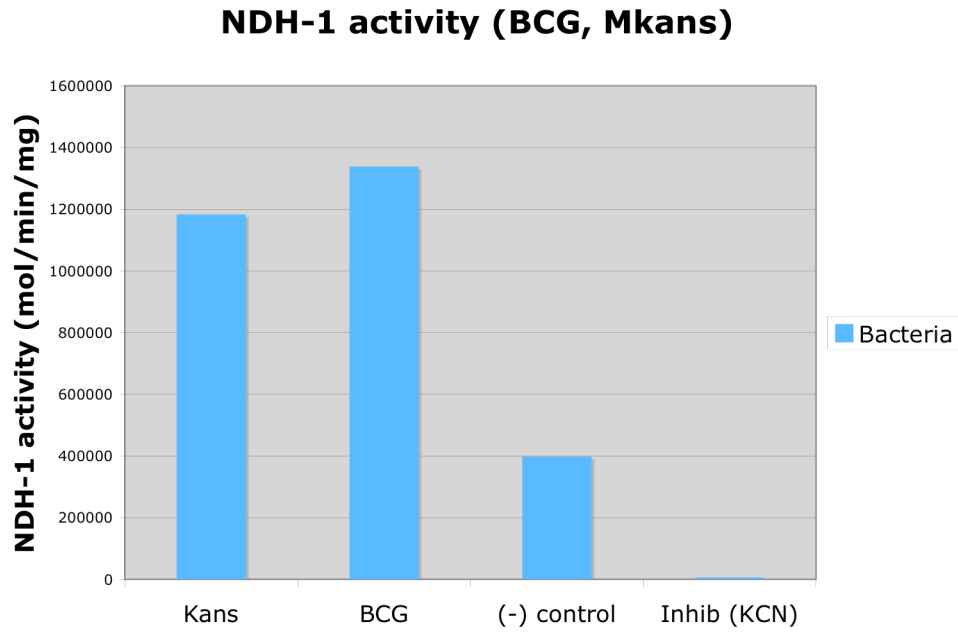


Figure 10. NDH-1 activity was calculated for BCG, Mkans, neg. control, and the inhibitor (KCN). The activity was calculated by dividing the kinetic slopes shown in figure with the multiplicity of the DCIP extinction co-efficient and the protein concentration.

Figure 11

NDH-1 assays of Msmeg, Msmeg+nuoG, Msmeg+J21

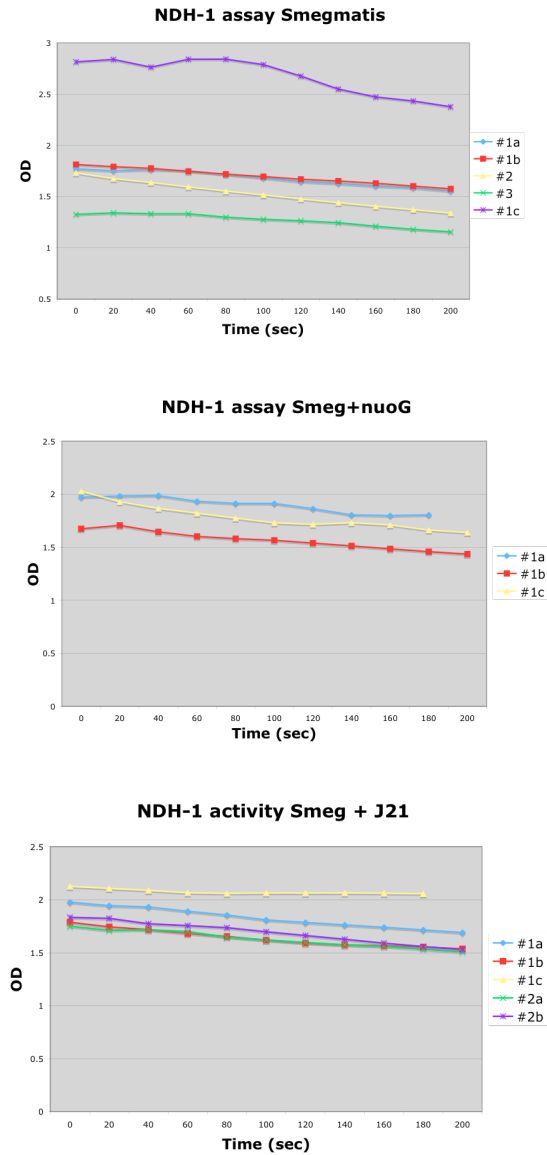


Figure 11. Kinetic slopes for NDH-1 assays are shown as reduction of OD over time. Kinetic slopes were measured following the addition of the DCIP substrate to Msmeg, Msmeg+nuoG, and Msmeg+J21. Different colored lines indicate separate reactions and different numbers indicate separate membrane isolations for the bacteria.

Figure 12

Comparing NDH-1 activities of Msmeg, Msmeg+nuoG, Msmeg+J21

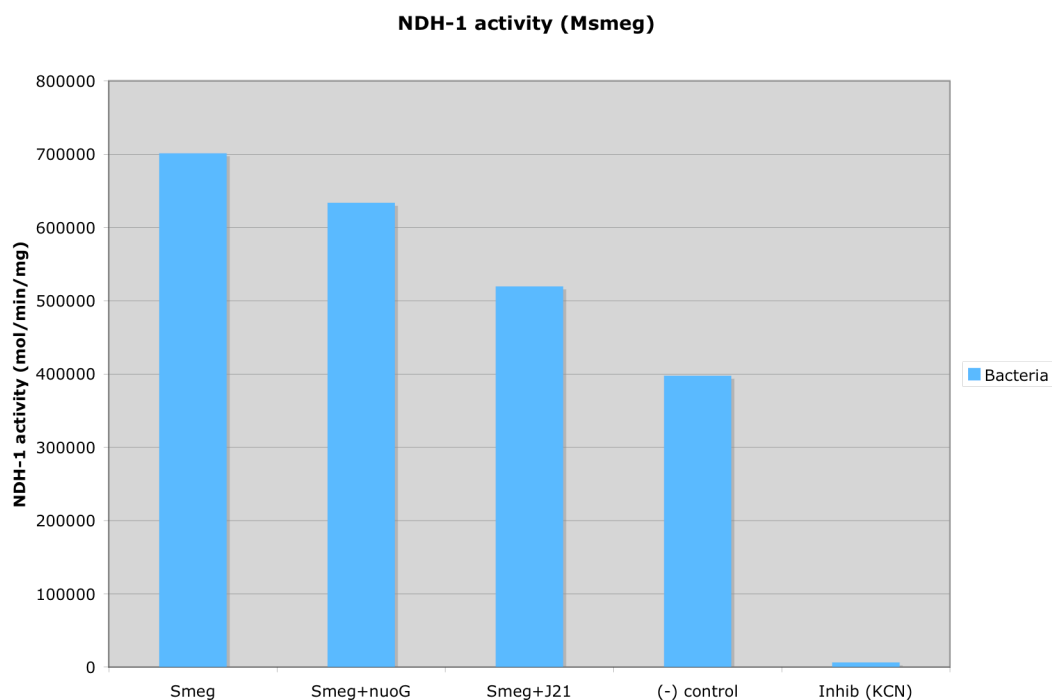


Figure 12. NDH-1 activity was calculated for Msmeg, Msmeg+nuoG, Msmeg+J21, neg. control, and the inhibitor (KCN). The activity was calculated by dividing the kinetic slopes shown in figure with the multiplicity of the DCIP extinction co-efficient and the protein concentration.

Figure 13

Comparing levels of NDH-1 activity in different mycobacterial species

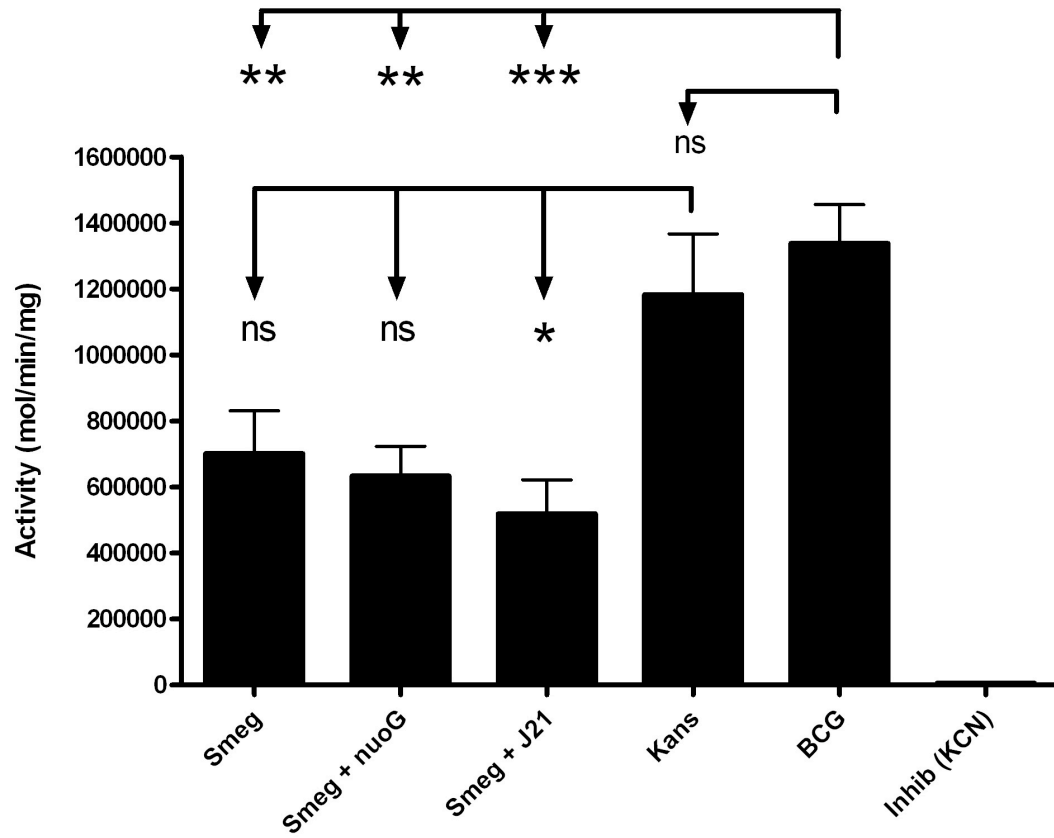


Figure 13. NDH-1 activity was calculated for Msmeg, Msmeg+nouG, Msmeg+J21, BCG, Mkan, neg. control, and the inhibitor (KCN). The activity was calculated by dividing the kinetic slopes shown in figure with the multiplicity of the DCIP extinction co-efficient and the protein concentration.

Figure 14

NDH-2 activity for Mkans, BCG, and neg. control

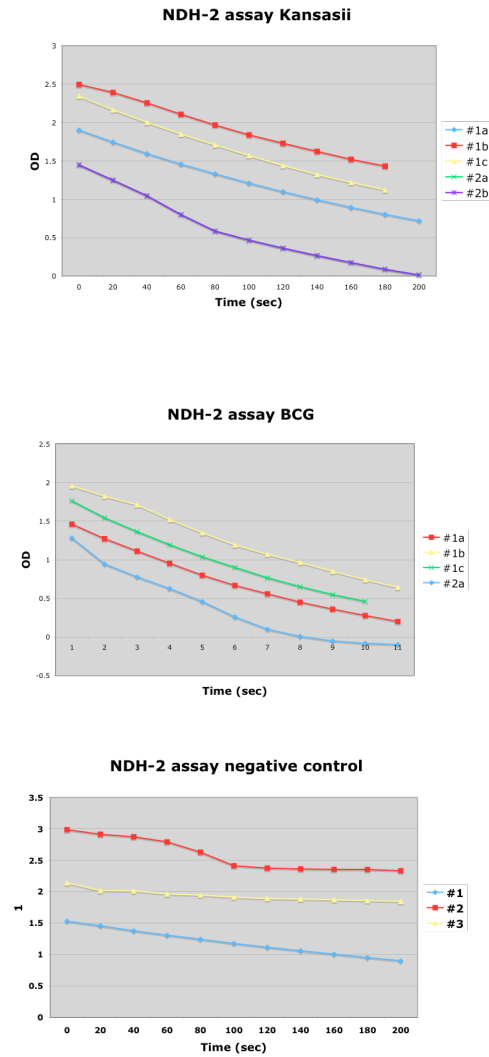


Figure 14. Kinetic slopes for NDH-2 assays are shown as reduction of OD over time. Kinetic slopes were measured following the addition of the DCIP substrate to BCG, Mkans, and neg. control. Different colored lines indicate separate reactions and different numbers indicate separate membrane isolations for the bacteria.

Figure 15

NDH-2 activities of Msmeg, Msmeg+nuoG, Msmeg+J21

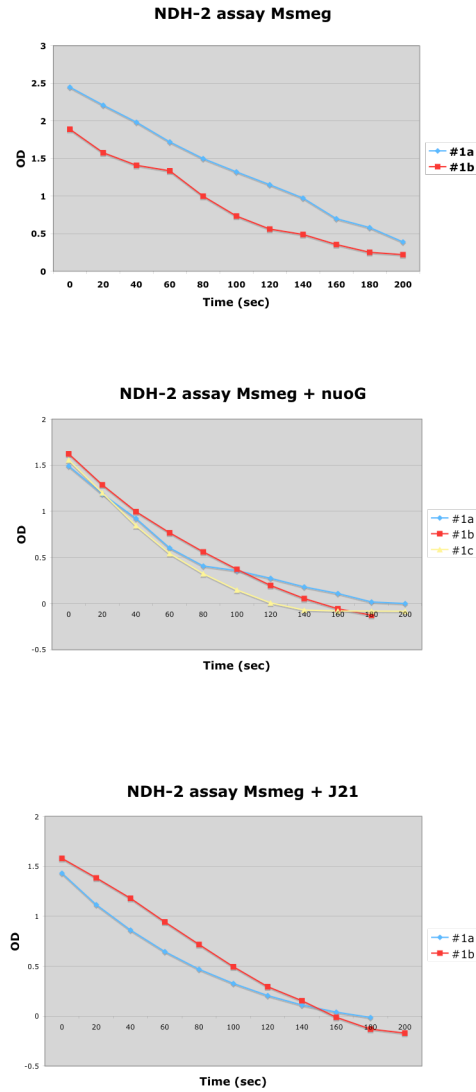


Figure 15. Kinetic slopes for NDH-2 assays are shown as reduction of OD over time. Kinetic slopes were measured following the addition of the DCIP substrate to Msmeg, Msmeg+nuoG, and Msmeg+J21. Different colored lines indicate separate reactions and different numbers indicate separate membrane isolations for the bacteria.

Figure 16

Comparing levels of NDH-2 activity in different mycobacterial species

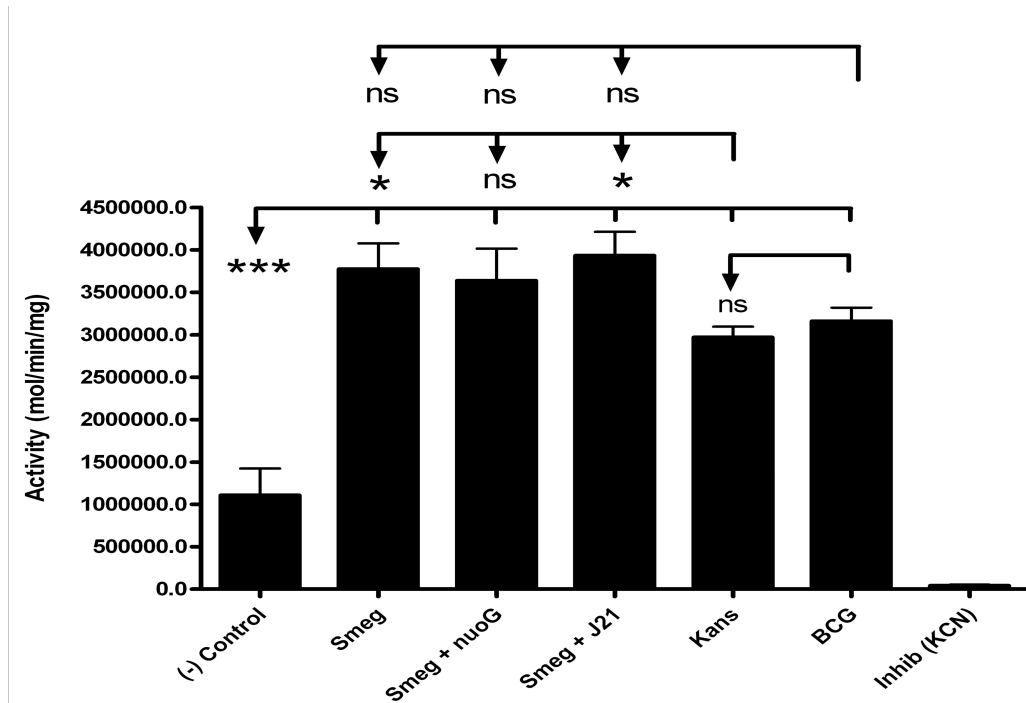


Figure 16. NDH-2 activity was calculated for Msmeg, Msmeg+nouG, Msmeg+J21, BCG, Mkans, neg. control, and the inhibitor (KCN). The activity was calculated by dividing the kinetic slopes shown in figure with the multiplicity of the DCIP extinction co-efficient and the protein concentration.

Creation of Myc-tagged and un-tagged NuoG plasmids

In order to conduct future studies regarding the correlation of NuoG from different *mycobacteria* and NDH-1 enzymatic activity, Myc-tagged NuoG and untagged NuoG pmv261 plasmids were created with *nuoG* from Mtb, BCG and Msmeg (Figure 17). The protein products of the myc-tagged plasmids were verified in a western-blot using anti-myc antibodies. Topo vector *nuoG* plasmids of all the above *myc*-tagged and untagged *nuoG* genes were created, in addition to the Mkans untagged *nuoG* plasmid (material and methods).

Creation of BCG Δ *nuoG* bacteria transformed with Myc-tagged NuoG plasmids

The plasmids mentioned above were used for transformation into competent BCG Δ *nuoG*, to study potential “gain of function” phenotypes. Glycerol stock were made and stored at -80°C for future apoptosis and NDH-1 activity assays.

Creation of Mtb Δ *nuoG* bacteria transformed with Myc-tagged NuoG plasmids

Mtb *nuoG*-myc plasmids from two separate preps (#2, #3) were electroporated into Mtb Δ *nuoG* bacteria that were made competent. Western blot revealed that the proteins extracted from the bacteria expressed the Mtb NuoG-Myc proteins (Figure 19). Glycerol stock were made and stored at -80°C for future apoptosis and NDH-1 activity assays, to test for “gain-of-function” phenotypes.

Creation of plasmids for full-length and partial Mtb NuoG antibody production

In order to study the potential role of *nuoG* in apoptosis inhibition, separate from its role as an NDH-1 subunit, an antibody against NuoG is needed for localization studies. The cloning of the plasmids for the Mtb NuoG-full length and the Mtb NuoG-short proteins were completed (material and methods). The short Mtb NuoG antibody will be used against different mycobacterial NuoG proteins, as the first 250 amino acids are conserved among mycobacterial species. The cloning was performed using a pet28c vector (Figure 18), and were sequence verified.

Figure 17

Map of the Mtb-*nuoG* antibody plasmid

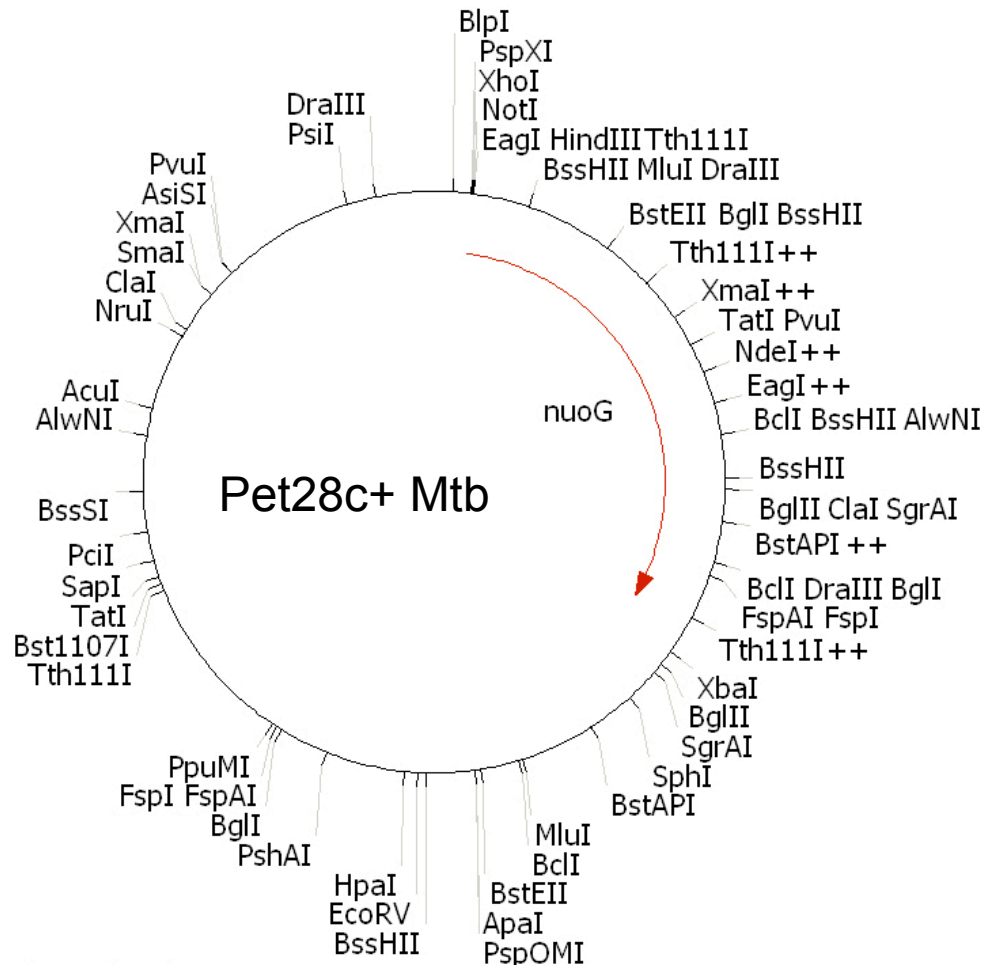


Figure 17. The Mtb *nuoG* was directionally cloned into the multiple cloning site of the pet28C vector. The region of the first 250 amino acids of the Mtb *nuoG* was similarly cloned into the pet28C vector (not shown).

Figure 18

nuoG-myc genes in pmv261

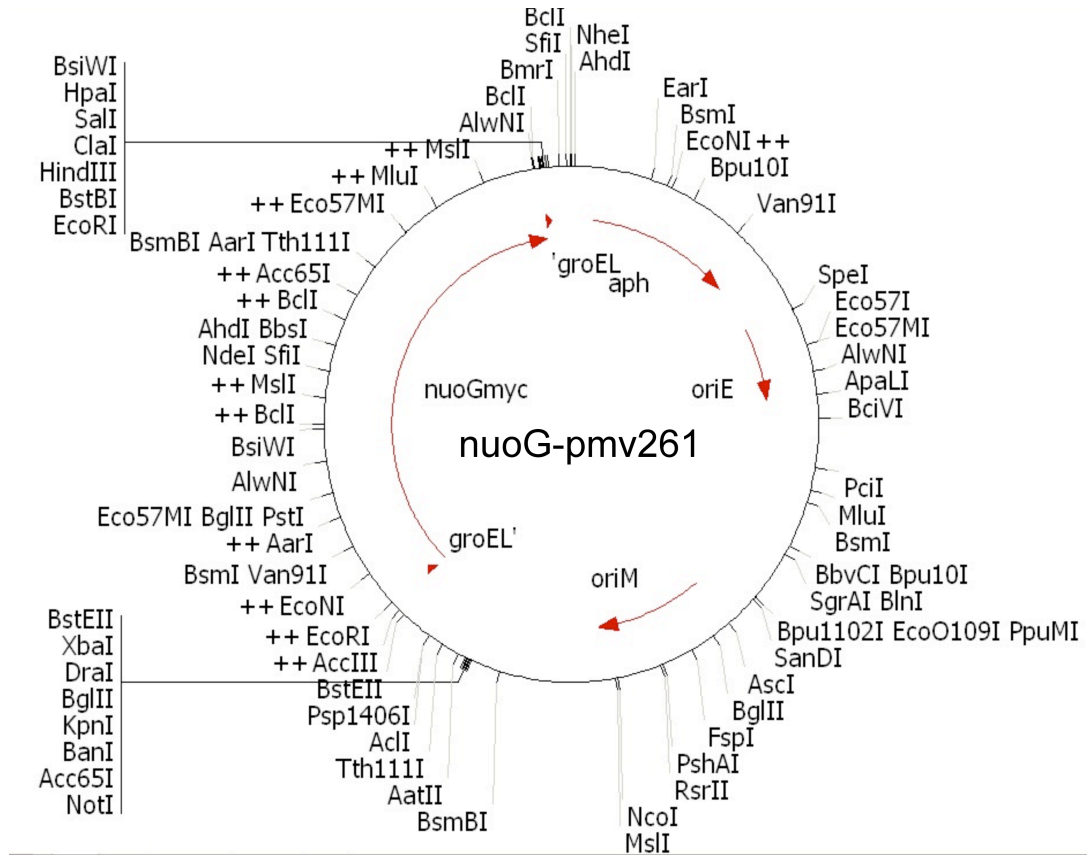


Figure 18. The *nuoG* genes of Mtb, BCG and Msmeg were cloned into the non-integrating pmv261 vector, both with *myc* tags and without them. The vector has a *groEL* promoter, a mycobacterial origin of replication (*oriM*) and an *E.coli* origin of replication (*oriE*).

Figure 19

Mtb NuoG-Myc proteins are expressed in Mtb Δ nuoG

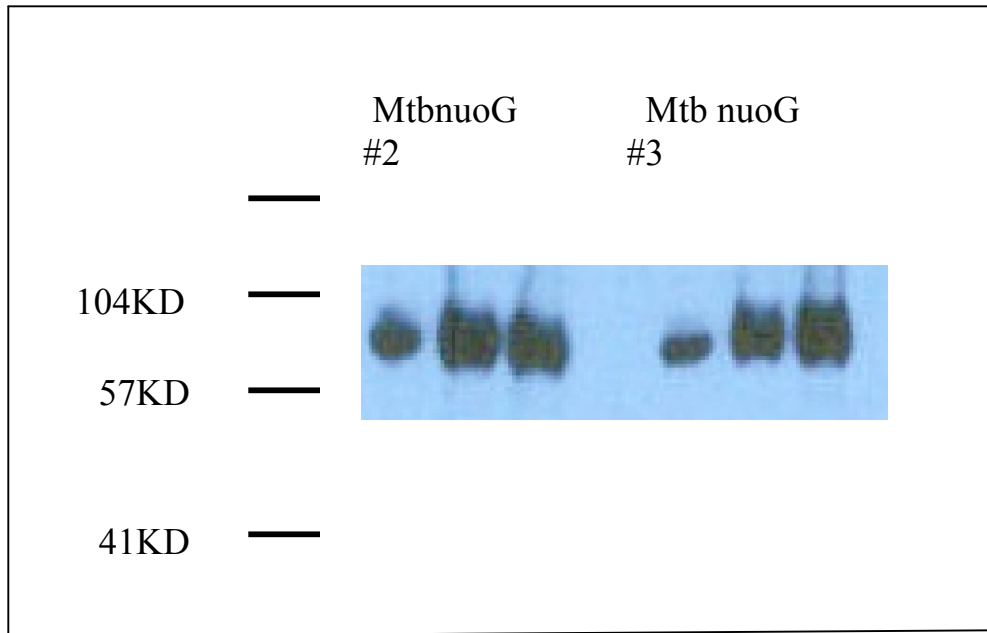


Figure 19. *Mtb nuoG-myc* plasmids from two separate preps (#2, #3) were electroporated into *Mtb Δ nuoG* bacteria that were made competent. The bacteria were grown on 7H10 agar plates with hygromycin (for selection of the *Mtb Δ nuoG*) and kenamycin (for selection of the *pmv261* containing bacteria). Colonies were grown in 7H9 media with the antibiotics. Proteins were extracted and used for immunoblotting. 10, 20 and 30 μ l of the protein extractions were loaded on a gel alongside a protein ladder. NuoG weighs approximately 94KDa.

Chapter 3: Discussion

In my research, I have examined the correlation of enzymatic activity of NDH-1 and anti-apoptotic capacity/virulence of *nuoG* in *Mycobacteria*. Currently, it is not possible to conclude with certainty the mechanism of apoptosis inhibition by *nuoG*. The working model of the Briken lab, which hypothesizes that it is the enzymatic activity of the NDH-1 complex that inhibits apoptosis, was not proven by this study. The idea that the facultative pathogenic *M. kansasii* and the non-pathogenic *M. smegmatis* didn't have functioning NDH-1 complexes and therefore could not inhibit apoptosis like the pathogenic BCG and *M. tuberculosis*, was contradicted by the NDH-1 activity assays. The level of NDH-1 activity of *M. kansasii* was comparable to that of BCG. The level of NDH-1 activity of *M. smegmatis* was only about 30% lower than that of BCG. Experiments using *M. tuberculosis* were not possible due to the fact that the French Press causes aerosolization of bacteria and cannot be used under Bio-Safety Level 3 conditions. Since the *NuoG* protein sequences of BCG and *M. tuberculosis* are almost identical it is safe to conclude that the BCG results would be the same for *M. tuberculosis*.

Previous studies showed that transforming *M. smegmatis* with the J21 cosmid causes significant reduction in apoptosis. It would have been expected that the NDH-1 activity of the transformed *M. smegmatis* would be significantly higher than that of the wild type *M. smegmatis*, if in fact the enzymatic activity were related to apoptosis inhibition. However, the results didn't show an increase, but a small, statistically insignificant decrease in activity. The J21 cosmid contains the 7/10 region which is involved in apoptosis inhibition, in addition to the *nuo* operon. The enzymatic activity assay implies that perhaps the 7/10 region is responsible for the anti-

apoptotic phenotype in Msmeg transformed with J21. However, Mkans transformed with only the *nuoG* plasmid also showed apoptosis inhibition (Velmurugan 2007), indicating *nuoG* alone is sufficient for apoptosis inhibition in Mkans. In studies conducted in Msmeg, however, the wild type Msmeg, the Msmeg with the J21 cosmid, and the Msmeg with the *nuoG* plasmid all had similar enzymatic activities.

The activity of the NDH-2 complexes was used as a control. All the bacteria that were compared for their NDH-1 activities showed similar NDH-2 activities. The NDH-2 activities were significantly higher than the NDH-1 rates. This was expected since NDH-2 is only one protein and not a protein complex like NDH-1, and therefore a lot less fragile when subjected to the isolation procedure. Also, NDH-2 is non-proton pumping and its rate might therefore be higher than that of NDH-1.

The working model investigated in my lab suggests the novel function of apoptosis inhibition for the NDH-1 complex in addition to its function in respiration. It also suggests a novel function for the NOX2 complex. If the model is accurate, the NOX2 generated ROS serve as sensors in the macrophages for the presence of intracellular pathogens that remain alive. This is supported by the fact that more and more NOX2 evasion strategies are being revealed in intracellular pathogens.

However, if enzymatic activity is not related to anti-apoptotic capacity, the NuoG subunit of the complex could have an independent mechanism by which it inhibits apoptosis. If that is the case then *nuoG* directly effects cell signaling towards survival. It is possible it affects the extrinsic apoptosis pathway (caspase 8

mediated) by effecting TNF α secretion or TNF α binding to its receptor. It is also possible that it neutralizes ROS directly, by its ability to accept electrons.

To investigate whether the enzymatic activity is correlated to apoptosis inhibition, it would be interesting to investigate a different NDH-1 mutant. The Briken lab is in the final steps of generating a BCG *nuoLM* deletion mutant. The L and M subunits of the complex are the proton translocators, therefore deleting them should abolish the enzymatic activity on the NDH-1 complex. If the mutant shows very low levels of NDH-1 activity (like the BCG *nuoG* mutant showed), as well as induction of high levels of apoptosis, the enzymatic correlation to apoptosis will be supported. However, if the mutant shows very low levels of NDH-1 activity, but low rates of apoptosis similar to the low rates in wild type BCG, then the enzymatic correlation to apoptosis will be contradicted. Another experiment that would be helpful would be to test the levels of apoptosis in cells infected with Msmeg transformed with only the Mtb*nuoG* plasmid. It would be interesting to see if apoptosis would be inhibited even though the enzymatic activity didn't change. It would also be interesting to study the levels of enzymatic activity and apoptosis in Mkans transformed only with the Mtb *nuoG* plasmid. The Mkans with the Mtb *nuoG* plasmid are currently being grown in the lab and will be ready for use in the near future.

The *nuoG* plasmids created in this study should prove very useful for future “gain-of-function” studies. Wild type bacteria, but especially the Mtb and BCG *nuoG* deletion mutants can be transformed with the plasmids and tested for NDH-1 activity and apoptosis inhibition, to search for correlation or lack of correlation.

The NuoG antibody, once produced, will be important for localization assays, especially if NuoG proves to function as an independent protein that effects host cell signaling. Finally, gold labeling followed by Electron microscopy would show if the NDH-1 complexes are located in proximity to the NOX2 complexes, and could support the correlation between the pumping of protons and subsequent neutralization of ROS, and inhibition of host cell apoptosis.

In conclusion, NuoG inhibits apoptosis in host cells either via its function as an NDH-1 subunit, or directly via effecting host cell signaling towards cell survival. Further studies are needed in order to support the current working model in the Briken lab, or to uncover a different mechanism for the inhibition of apoptosis by *nuoG*. In my project, I have established an assay and made the constructs required for investigating NDH-1 activities in different mycobacterial species. My results demonstrate previously unknown enzymatic activities of the different wild type bacteria and transformed bacteria. Using my data, the established assay and the constructs, it will be possible to complete the puzzle of whether NDH-1 enzymatic activity correlates with apoptosis inhibition.

Chapter 4: Experimental procedures

Bacterial and culture conditions

M. smegmatis (mc²155), *M. kansasii* (Hauduroy ATCC 12478) and Mtb (H37Rv ATCC 25618) were obtained from the American Type Culture Collection. *M. bovis* BCG Pasteur strain was obtained from the Trudeau Culture Collection (Saranac Lake, New York, United States). The cultures were grown in Middlebrook 7H9 broth (Difco) supplemented with 0.5% glycerol, 10% oleic acid-albumin-dextrose-catalase (Difco), and 0.05% TWEEN-80, or on Middlebrook 7H10 agar (Difco). For selective media, 50 µl hygromycin or 40 µl kanamycin were added.

Membrane isolations:

Mycobacterial cultures were grown in 7H9 media to OD(600nm)= 0.7-1.0 in 2 L Roller Bottles. Cultures were spun down at 4,000 rpm for 15 minutes. The cultures were washed twice with 50mL cold phosphate buffer (50 mM KH₂PO₄ pH 7.5, 5 mM MgSO₄). The pellet was weighed and recorded for later calculations. The pellet was re-suspended in 2 ml cold complete phosphate buffer containing DNase1(5,000 units, Roche), protease cocktail inhibitor solution (0.1 ml, Roche- dissolve in 1 ml TRIS-HCL) and soybean trypticase inhibitor (5 µl per 2 ml buffer). The cell suspensions were passed through a French Press (4 passages, 1000 psi/ cm²). The suspensions were spun to remove cell debris at 1,200 G for 20 minutes at 4 C°.

The membrane fractions were isolated by ultracentrifugation at 100,000 G for 90 minutes at 4 C°. The pellets were then re-suspend in 1 ml/gram pellet complete cold phosphate buffer. Protein concentrations were measured using the BCA assay kit.

NADH assays:

The rate of DCIP (2,6 dichlorophenolindophenol, 0.1 mM) reduction was measured at room temperature at 610 nm in the presence of NHDH (reduced nicotinamide hypoxanthine dinucleotide, 0.4 mM) in phosphate buffer. 20 ul of membrane isolation preps were used per assay. The reduction was measured for 200 seconds at 20 second intervals. The kinetic slope was calculated using the spectrophotometer's kinetic reaction function, and was indicated in centimeters per minute units. NADH activity was measured by dividing the kinetic slope by the multiplication of the DCIP extinction coefficient ($16.5 \text{ mM}^{-1} \text{ cm}^{-1}$) and the protein concentration. NDH-2 assays were performed similarly, replacing NHDH with NADH (reduced nicotinamide adenine dinucleotide).

Creating the *nuoG* plasmids

The *nuoG* genes of were PCR amplified include the up-stream Shine-Delgarno sequences and the downstream myc tag. The primers used were:

For Mkan- Forward primer: CGAATACGTCGCGCATGTTCG.

Reverse primer: GAGTACGACTGGCAGGACCA.

For Mtb and BCG- Forward primer: CCTGGCCCACGTCGAAGGAG.

Reverse primer without adding myc tag: TGTCGGCGTACTGGGGGCAC.

Reverse primer adding a myc tag: TCACAGGTCCTCCTCGCT

GATCAGCTTCTGCTCTAATGAGCCCGCTCCGATTT.

For Msmeg- forward primer: TGGCCGAACCGACCAAGGAC.

Reverse primer without adding myc tag: GAGCATGAGCCACCACGGATCG.

Reverse primer adding a myc tag: TCACAGGTCCTCCTCGCTGATCAGCTT

CTGCTCTAATGCCCGGCTCCGATCG.

The stop codons were altered from TGA to TTA (leu). Blunt-end cloning was initially performed to clone the gene into the sequencing topo vector. The sequences of the plasmids were verified. The genes were digested out of the topo vector using the EcoRI enzyme at 37 C°, ran on a gel, then gel purification. The gene was ligation into the mycobacterial non-integrating pmv261 vector. Restriction enzyme digestion was performed to verify orientation of the insert.

Plasmid sequencing:

PCR amplification of the plasmids was performed with sequencing primers and Big Dye Terminator buffer and enzyme. The sequencing primers used were the commercial topo vector sequencing primers M13F and M13R. Following the PCR, 40 µl of 75% isopropanol were added to each sample and gently vortexed. The samples were incubated at room temperature for 15 minutes. The samples were centrifuged for 30 minutes at 3770 revolutions per minute (RPM). The samples were decanted onto a paper towel and immediately spun at 2330 RPM for one minute. 75 µl of 70% isopropanol were added to each sample and gently vortexed.

The samples were centrifuged for 10 minutes at 3770 RPM. The samples were decanted onto a paper towel and immediately centrifuged at 2230 RPM for one minute. Samples were re-suspended in 10 μ l HiDi formamide and vortexed. Samples were heated at 95 C° for two minutes then chilled on ice for five minutes. 10 μ l of each sample were loaded onto the sequencing plate, and loaded into the ABI 3100 sequencer.

Introducing the *nuoG* plasmids into competent mycobacteria:

50 ml of *M. Smeg* was grown to an O.D 600 of 0.5-1. The entire procedure is temperature sensitive and was performed in 4 °C (on ice). The culture was spun down (3,000 rpm, 10 minutes), washed 3 times with 10% glycerol/ 0.05% Tween-80. The pellet was taken up in 4 ml wash buffer, and was used immediately. 5 μ l of the selected plasmids were placed in a biorac cuvette, with 400 μ l of the competent *smegmatis*. The cells were electroporated at 2.5 kV, 25 μ FD, 1000 Ω . The cells were immediately transferred to a round bottom PP tube containing 2 ml of medium without antibiotic. The culture was then incubated for 2 hours, shaking at 37 °C. *Mtb nuoG-myc* plasmids from two separate preps (#2, #3) were electroporated into *Mtb Δ nuoG* bacteria that were made competent. The bacteria were grown on 7H10 agar plates with hygromycin (for selection of the *Mtb Δ nuoG*) and kenamycin (for selection of the *pmv261* containing bacteria).

Creating anti-NuoG antibody

Antibody is being created against the region of NuoG similar among strains (first 250 amino-acids), as well as against the full length Mtb NuoG. Primers were designed without a start codon (which is present in the plasmid), and with restriction enzyme sites that will allow directional cloning into pet28c vector. Once the PCR from J21 is amplified according to this method, the fragment is ligated into pet28C and transformed in competent *E. coli* cells. The plasmid will then will be propagated in *BL21-DE3* cells. Once the culture is IPTG induced, and plasmids containing the insert are selected, a larger culture is grown (10 ml).

The protein is purified using glass-beads, and the total protein runs on a coomassie-blue gel. NuoG is cut out of the gel, and his-tagged NuoG (which is the mycobacterial protein, not the *E. coli* protein) is purified using a his-column. The his tag is cleaved using the thrombine site, and the protein can be sent out to make polyclonal antibodies against. These antibodies will be affinity purified for NuoG specificity.

Mycobacterial protein extraction

10 ml cultures were grown from colonies of Mtb containing the *nuoG-myc* plasmids to an OD₆₀₀ of 0.7. The culture was centrifuged at 2,000 X g for 20 minutes to pellet the bacteria. The pellet was washed once with 10 ml phosphate-buffered saline (PBS). Following additional centrifugation, the supernatants were discarded and 10 ml of ice-cold PBS was added to the cell pellet. The pellets were vortexed until resuspended, then spun for 10 minutes at 2,000 X g. The supernatants

were discarded and the cell pellet was resuspended in 1.5 ml ice-cold PBS. Cell pellets were vortexed until resuspended. The cell suspensions were transferred to a 2 ml screw-cap tube. Tubes were spun for 10 minutes in a microcentrifuge. The supernatants were discarded and the cell pellets were resuspended in 500 μ l of extraction buffer. 100 μ l glass beads were added to the cells (106 μ m glass beads, Sigma). The cells with the beads were vortexed at top speed for five minutes. The supernatant was collected and transferred into a new tube, and 100 μ l of 5 X SDS-PAGE sample buffer was added to each tube, and mixed by vortexing. The samples were incubated at 100 for 10 minutes. The samples were then moved from the Bio safety level (BSL)-3 lab to the BSL-2 lab, and immunoblotting assays were then performed.

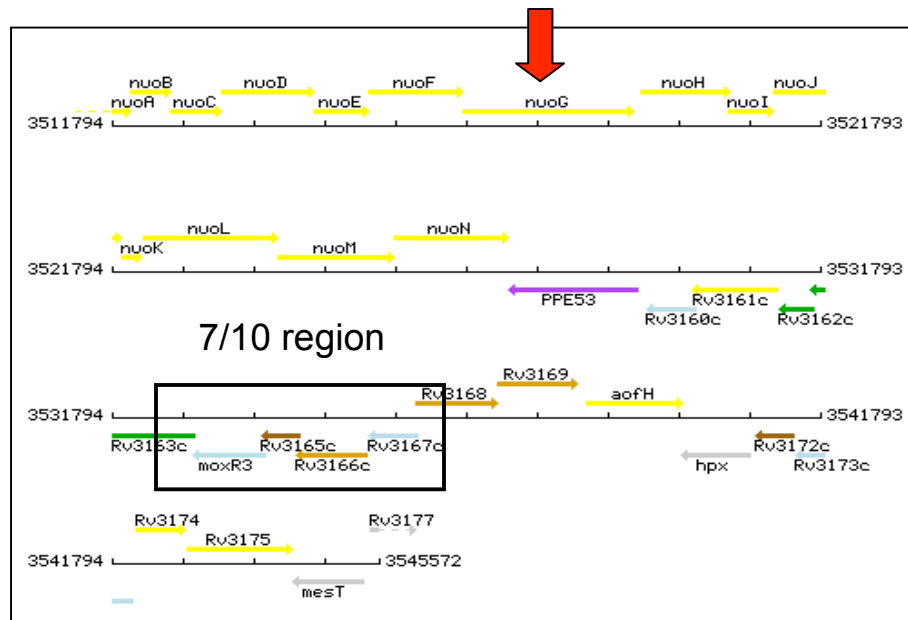
Immunoblot analysis of mycobacterial proteins

10% HEPES gels were loaded with 10, 20 and 30 μ l of protein samples and 5 μ l of protein ladder. The gel ran at 100 volt for 40 minutes in Hepes buffer. The gel was transferred onto an activated PVDF membrane (pre-immersed in 100% methanol, washed in transfer buffer) for one hour at 12 volts. The membrane was briefly washed in 0.05% tween-PBS buffer. The membrane was blocked in 5% milk in PBS for 15 minutes at room temperature. The membrane was washed for 15 minutes with 0.05% tween-PBS, three times. The membrane was incubated with the mouse anti-myc primary antibody (9E10, development studies hybridoma bank, developed at the University of Iowa) for one hour at room temperature. The membrane was washed for fifteen minutes with 0.05% tween-PBS, three times. The

membrane was incubated with the secondary goat-anti-mouse antibody for one hour at room temperature. The membrane was washed for five minutes with 0.05% tween-PBS, five times. The membrane was then incubated in a 1:1 dilution of Luminol peroxidase buffer. The membrane was exposed for one minute on a film and then developed.

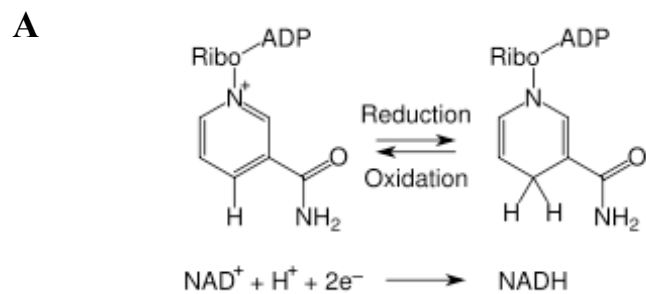
Appendix 1

The J21 cosmid



Appendix 1. The J21 cosmid includes almost the entire *nuo* operon, as well as the 7/10 region.

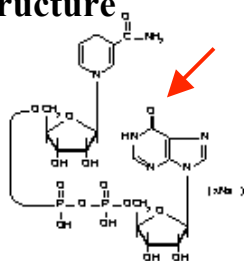
Appendix 2



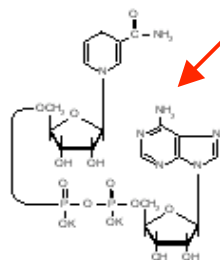
B

NHDH

structure



NADH



Appendix 2. NADH reduction reaction (A). The difference in structures between NHDH and NADH (B).

Bibliography

Abramovitch R, Martin G. Strategies used by bacterial pathogens to suppress plant defenses. *Curr. Opin. Plant Biol* 2004; 7: 356-364.

Barnes P, Modlin R, Ellner J. Tuberculosis; pathogenesis, protection and control. ASM Press 1994. 417-430.

Bardarov S, Bardarov Jr., Pavelka M, Sambandamurthy V, Larsen M, et al. Specialized transduction: an efficient method for generating marked and unmarked gene disruptions in *Mycobacterium tuberculosis*, *M. bovis* BCG and *M. smegmatis*. *Microbiology* 2002; 148: 3007-3017.

Behr M, et al. Comparative genomics of BCG vaccines by whole-genome DNA microarray. *Science* 1999; 284: 1520-1523.

Braumstein M, et al. Identification of genes encoding exported *Mycobacterium tuberculosis* proteins using Tn552'phoA in vitro transposition system. *J Bacterial* 2000; 182: 2732-2740.

Braunstein M, Espinosa B, Chan J, Belisle J, Jacobs W. SecA2 functions in the secretion of superoxide dismutase A and in the virulence of *Mycobacterium tuberculosis*. *Mol. Microbiol.* 2003; 48: 453-464.

Briken V, Miller J. Living on the edge: inhibition of host cell apoptosis by mycobacterium tuberculosis. *Future Medicine* 2008; 4: 4.

David P, Baumann M, Wikstrom M, Finel M. Interaction of Purified NDH-1 from *Escherichia coli* with ubiquinone analogs. *Biochemica et Biophysica Acta* 2002; 1533: 268-278.

Dye C, Watt C, Bleed D, Hosseini S, Raviglione M. Evolution of tuberculosis control and prospects for reducing tuberculosis incidence, prevalence, and deaths globally. *JAMA* 2005; 293: 2676-2775.

Guermonpres P, Amigorena S. Pathways for antigen cross presentation. *Springer Semin. Immunopathol.* 2005; 26: 257-271.

Hingley-Wilson S, Sambandamurthy V, Jacobs W. Survival perspectives from the world's most successful pathogen, *Mycobacterium tuberculosis*. *Nature immunology* 2003; 4: 10.

Iriti M, Faoro F. Review of innate and specific immunity in plants and animals. *Mycopathologia* 2007; 164: 57-64.

Jayakumar D, Jacobs W, Narayanan S. Protein Kinase E of *Mycobacterium tuberculosis* has a role in the nitric oxide stress response and apoptosis in a human macrophage model of infection. *Cell. Microbiol.* 2007; 10 (2): 365-374.

Keane J, Remold H, Kornfeld H. Virulent *Mycobacterium tuberculosis* strains evade apoptosis of infected alveolar macrophages. *J. Immunol* 2000; 164: 2016-2020.

Klinger K, Tchou-Wong K, Brandli O, et al. Effects of mycobacteria on regulation of apoptosis in mononuclear phagocytes. *Infect. Immun.* 1997; 65: 5272-5278.

Miller B, et al. Mycobacteria inhibit nitric oxide synthase recruitment to phagosomes during macrophage infection. *Infect. Immun.* 2004; 72: 2872-2878.

Nguyen L, Pieters J. The Trojan horse: survival tactics of pathogenic mycobacteria in macrophages. *TRENDS in Cell Biology* 2005; 15: 5.

Pan H, Yan B, Rojas M, Shebzukhov Y, Zhouh et al. *Ipr1* gene mediates innate immunity to tuberculosis. *Nature* 2005; 434: 767-772.

Pethe K, et al. Isolation of *Mycobacterium tuberculosis* mutants defective in the arrest of phagosome maturation. *Proc. Natl. Acad. Sci.* 2004; 101: 13642-1347.

Placido R, Mancino G, Amendola A, et al. Apoptosis of human monocytes/macrophages in *Mycobacterium tuberculosis* infection. *J. Pathol* 1997; 181: 31-38.

Purdy G, Owens R, Bennett L, Russell D, Butcher B. Kinetics of phosphatidylinositol-3-phosphate acquisition differ between IgG bead-containing phagosomes and *Mycobacterium tuberculosis*-containing phagosomes. *Cell Microbiol* 2005; 7: 1627-1634.

Riendeau C, Kornfeld H. THP-1 cell apoptosis in response to mycobacterial infection. *Infect. Immune.* 2003; 71: 254-259.

Sazanov L, Hinchliffe P. Structure of hydrophilic domain of respiratory complex 1 from *Thermus thermophilus*. *Science* 2006; 311: 1430-1436.

Spratt J, Ryan A, Britton W, Triccas J. Epitope-tagging vectors for the expression and detection of recombinant proteins in mycobacteria. *Plasmid* 2005; 53: 269-273.

Schaible U, Winau f, Sieling P, et al. Apoptosis facilitates antigen presentation to T lymphocytes through MHC-1 and CD1 in tuberculosis. *Nat. Med.* 2003; 9: 1039-1046.

Stover C, de la Cruz V, Fuerst T, Burlein J, Benson L, et al. New use of BCG for recombinant vaccines. *Nature* 1991; 351: 456-460.

Velmurugan K, Chen B, Miller J, Azogue S, Gurses S, Hsu T, Glickman M, Jacobs W, Porcelli S, Briken V. *Mycobacterium tuberculosis* nuoG Is a Virulence Gene That Inhibits Apoptosis of Infected Host Cells. *PLoS Pathogens* 2007; 3: 7.

Walburger A, et al. Protein kinase G from pathogenic mycobacteria promotes survival within macrophages. *Science* 2004; 304: 1800-1804.

Yagi T, Yano T, Di Bernardo S, Matsuno-Yagi A. Prokaryotic complex I (NDH-1), an overview. *Biochimica et Biophysica Acta* 1998; 1364: 125-133.

Yagi T, Matsuno-Yagi A. The Proton Translocating NADH-Quinone Oxidoreductase in the Respiratory Chain: The Secret Unlocked. *Biochemistry* 2003; 42: 2266-2274.